Supporting Information

Broadband short-wave infrared phosphor $Mg_4Nb_2O_9:Cr^{3+},Li^+$ for nondestructive safety detection and biomedical imaging

Qingyang Ding,[1,a)] Jincheng Wu,[2,a)] Dechao Yu,[1,3,*] Xinxin Han,[3] Yayun Zhou,[4] Tiantian Shen,[1] Yunfeng Ma,[2,*] Songlin Zhuang[1] and Dawei Zhang[1]

[1]*Engineering Research Center of Optical Instrument and System, Ministry of Education and Shanghai Key Lab of Modern Optical System, University of Shanghai for Science and Technology, Shanghai 200093, People's Republic of China*

[2]*Institute of Crystal Growth, School of Materials Science and Engineering, Shanghai Institute of Technology, Shanghai 201418, China*

[3]*MOE Key Laboratory of New Processing Technology for Non-ferrous Metals and Materials, Guangxi Key Laboratory of Processing for Non-ferrous Metals and Featured Materials, Guangxi University, Nanning, Guangxi 530004, China*

[4]*Guangdong-Hong Kong-Macao Joint Laboratory for Intelligent Micro-Nano Optoelectronic Technology, School of Physics and Optoelectronic Engineering, Foshan University, Foshan 528225, China*

Corresponding authors:

*Dechao Yu. Email: d.yu@usst.edu.cn

*Yunfeng Ma. Email: yunfengma@sit.edu.cn

a) these authors contributed equally to this work

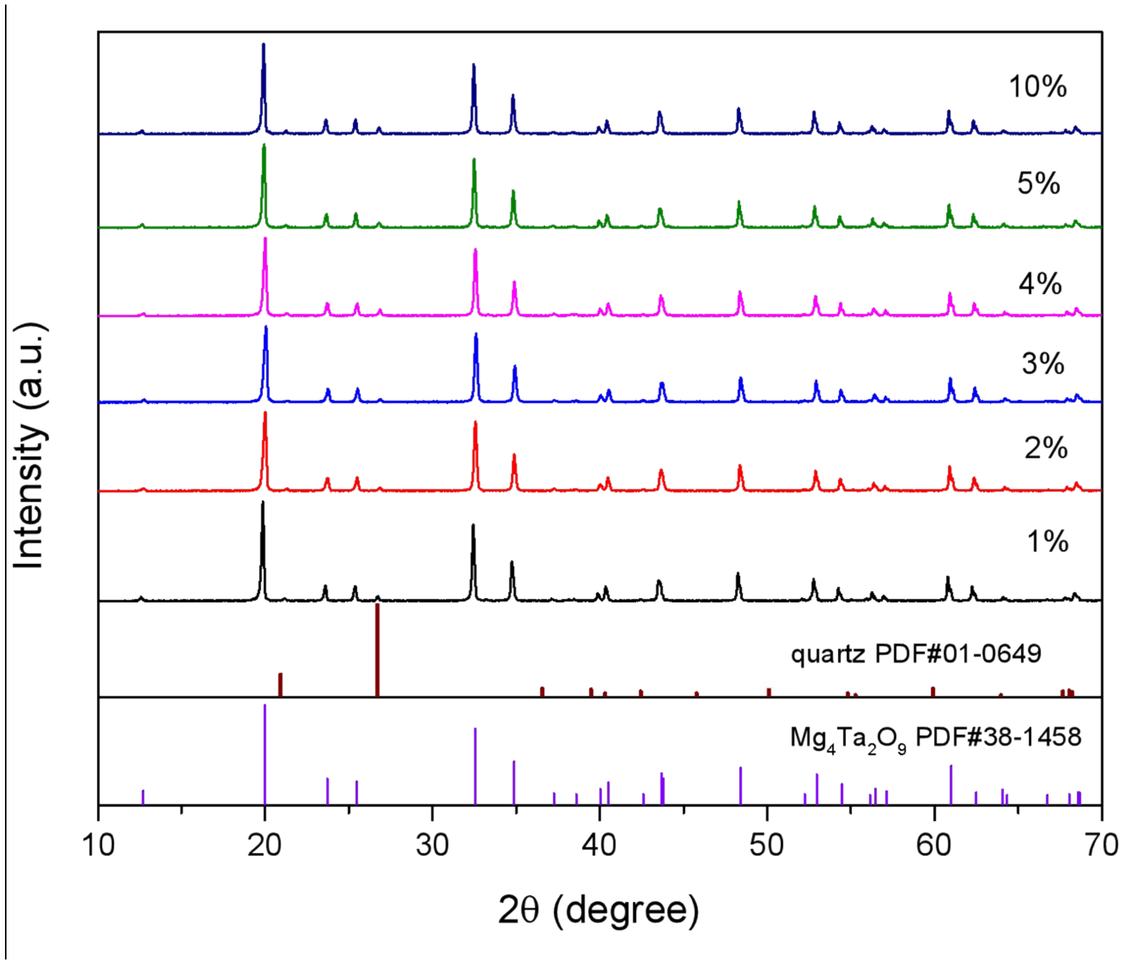

Fig. S1 Measured XRD patterns of $Mg_4Ta_2O_9$:x%Cr^{3+} (x = 1, 2, 3, 4, 5, 10) samples as well as the diffraction patterns of $Mg_4Ta_2O_9$ standard reference (PDF#38-1458). Noted that the two diffraction peaks at 21.11° and 26.61° just corresponds to the strongest peaks of quartz [PDF#01-0649, (100) at 20.885° and (101) at 26.587°] sheet used in the XRD measurements.

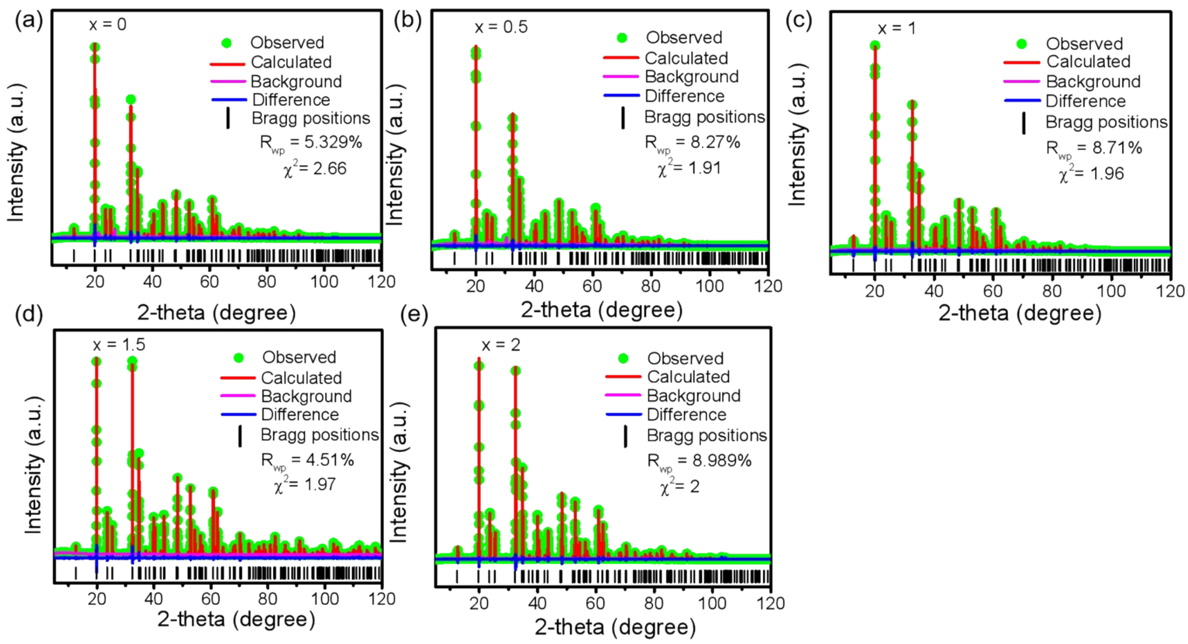

Fig. S2 Rietveld refinement XRD of $Mg_4Nb_xTa_{2-x}O_9$:3%Cr^{3+} (x = 0, 0.5, 1, 1.5, 2) phosphor samples, respectively.

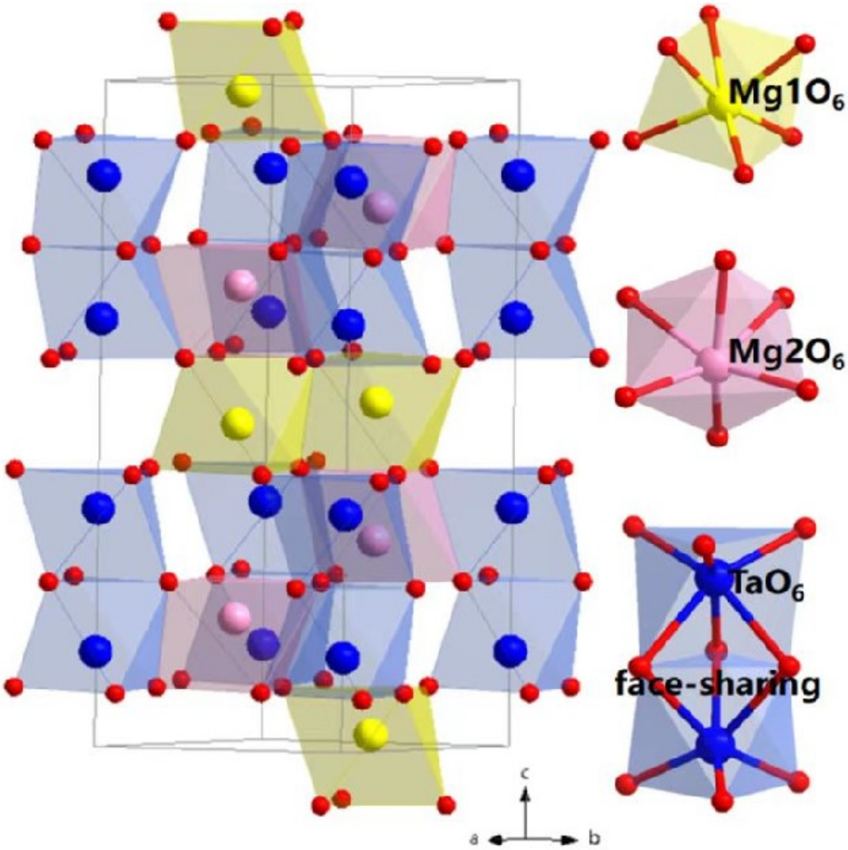

Fig. S3 The crystal structure of $Mg_4Ta_2O_9$ compound and the coordination environments

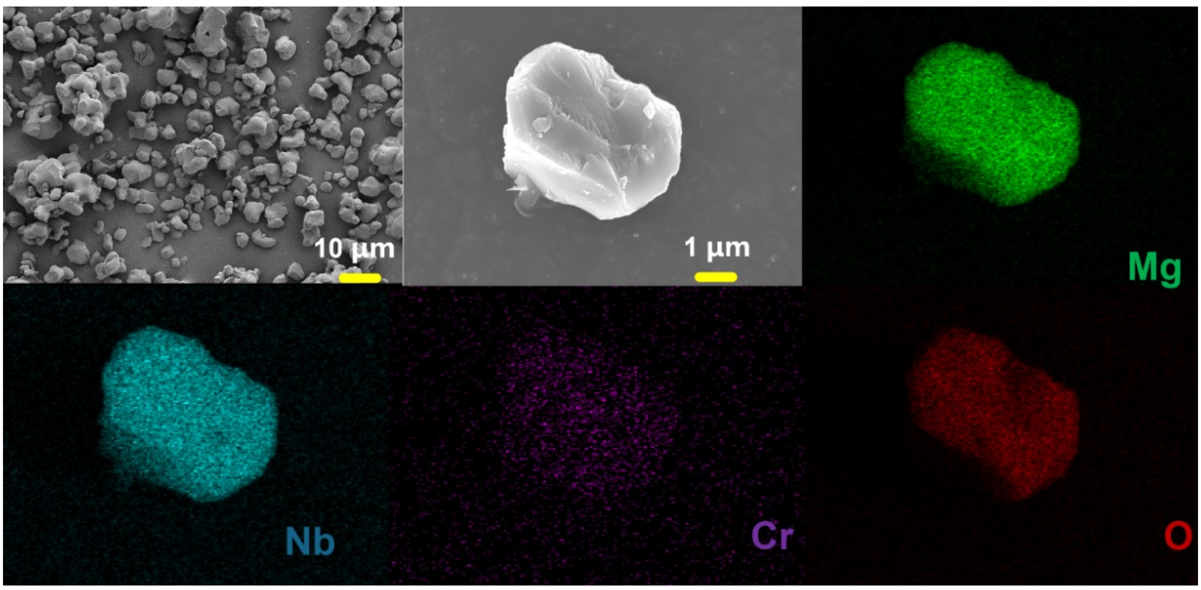

Fig. S4 SEM and EDS mapping images of the obtained $Mg_4Nb_2O_9$:3%Cr^{3+} powder sample

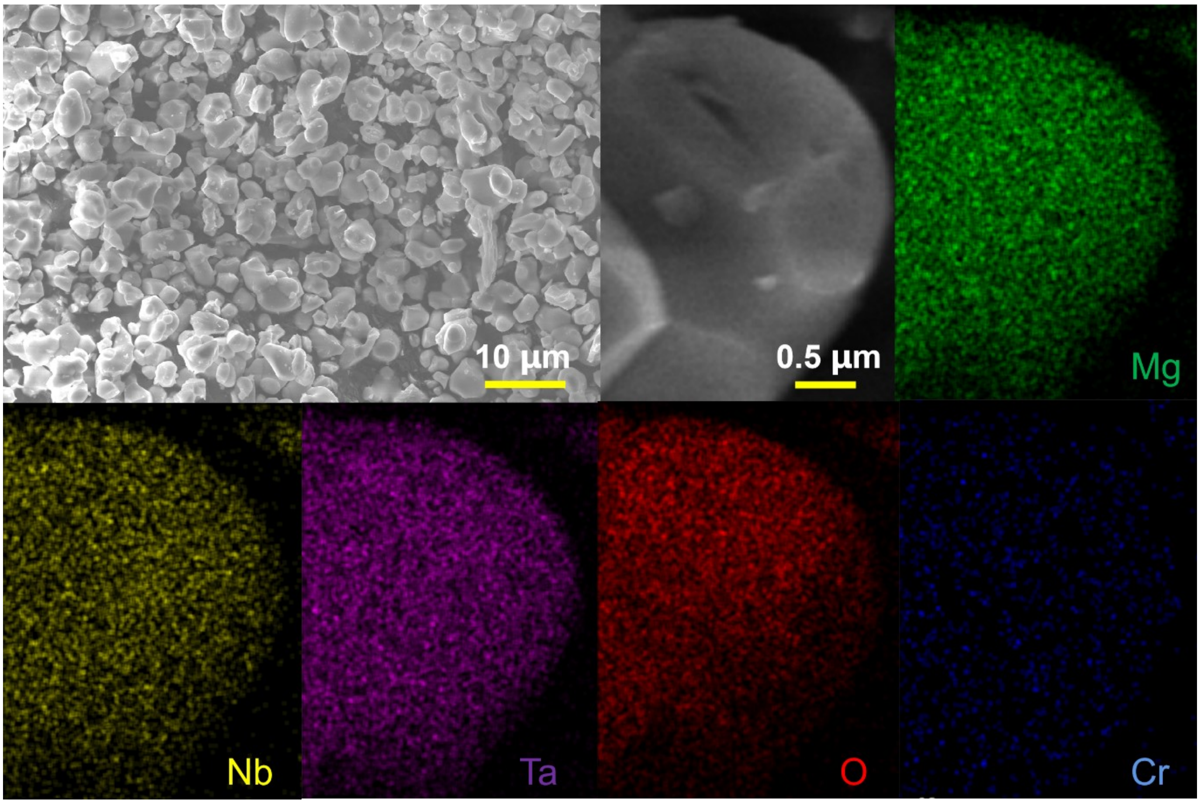

Fig. S5 SEM and EDS mapping images of the obtained Mg_4TaNbO_9:3%Cr^{3+} powder sample

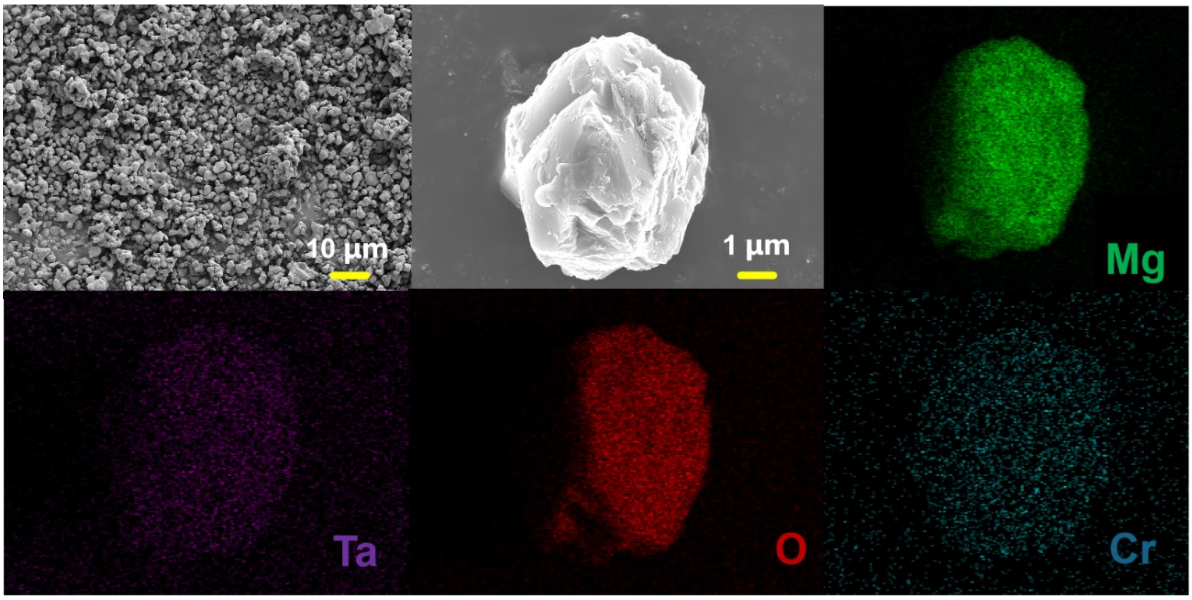

Fig. S6 SEM and EDS images of the obtained $Mg_4Ta_2O_9$:3%Cr^{3+} powder sample

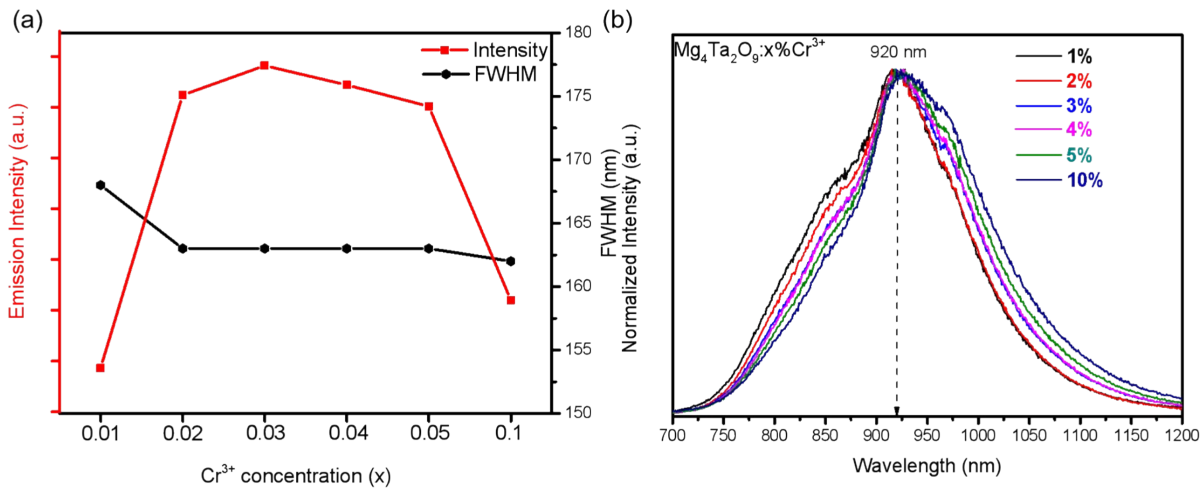

Fig. S7 (a) Cr^{3+} concentration-dependent emission intensities of $Mg_{4-x}Cr_xTa_2O_9$ (x = 0.01, 0.02, 0.03, 0.04, 0.05, 0.10) samples under excitation of 468 nm. (b) Normalized emission spectra of $Mg_4Ta_2O_9$:x%Cr^{3+} (x = 1, 2, 3, 4, 5, 10) samples under 468 nm excitation.

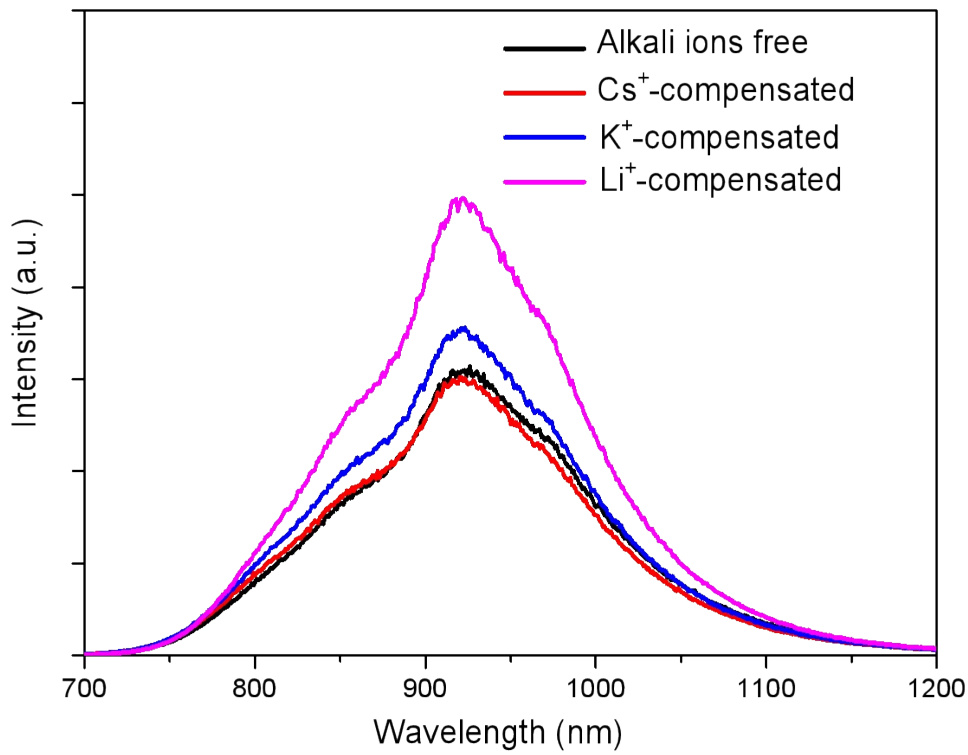

Fig. S8 Emission spectra of $Mg_4Ta_2O_9$:3%Cr^{3+} and $Mg_4Ta_2O_9$:3%Cr^{3+},M^+ (M = Li, K, Cs) under excitation of 468 nm. The same molar amount of alkali metal compounds, i.e. Li_2CO_3, K_2CO_3 and Cs_2CO_3, were also added during the synthesis of $Mg_4Ta_2O_9$:3%Cr^{3+} optimal phosphor, respectively. It can be seen that addition of Cs_2CO_3 does not increase the PL intensity, but the Li_2CO_3 and K_2CO_3 additives both work well. Particularly, the Li_2CO_3 plays the most effective charge compensation and/or fluxing actions.

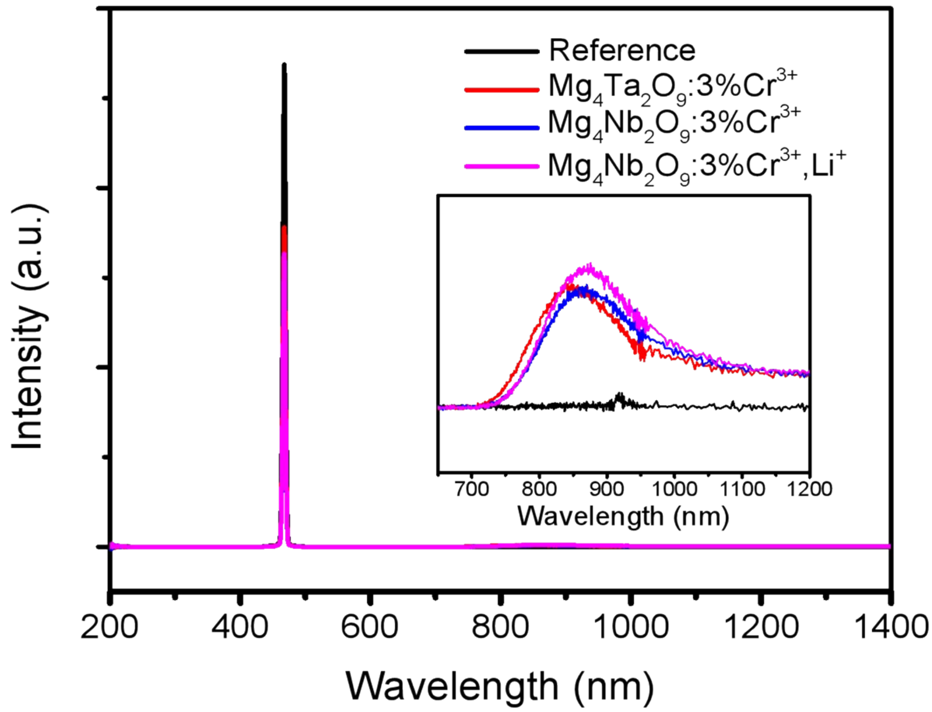

Fig. S9 Spectral curves of QE measurement for the $Mg_4Ta_2O_9$:3%Cr^{3+}, $Mg_4Nb_2O_9$:3%Cr^{3+} and $Mg_4Nb_2O_9$:3%Cr^{3+},Li^+ phosphor samples (λ_{ex} = 468 nm) by means of a Quantaurus-QY plus C13534-12 system (Hamamatsu Corp.).

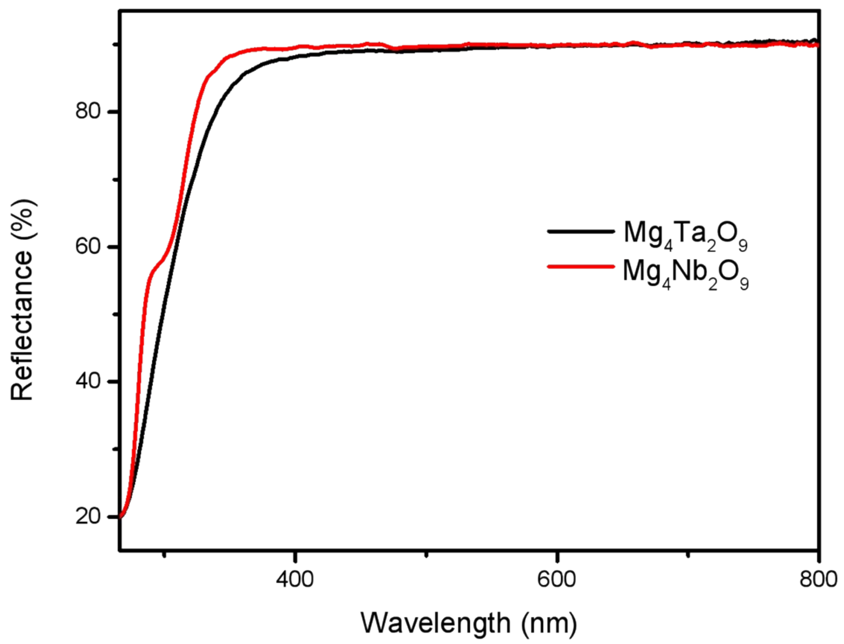

Fig. S10 Diffuse reflectance spectra of the prepared $Mg_4Ta_2O_9$ and $Mg_4Nb_2O_9$ host samples.

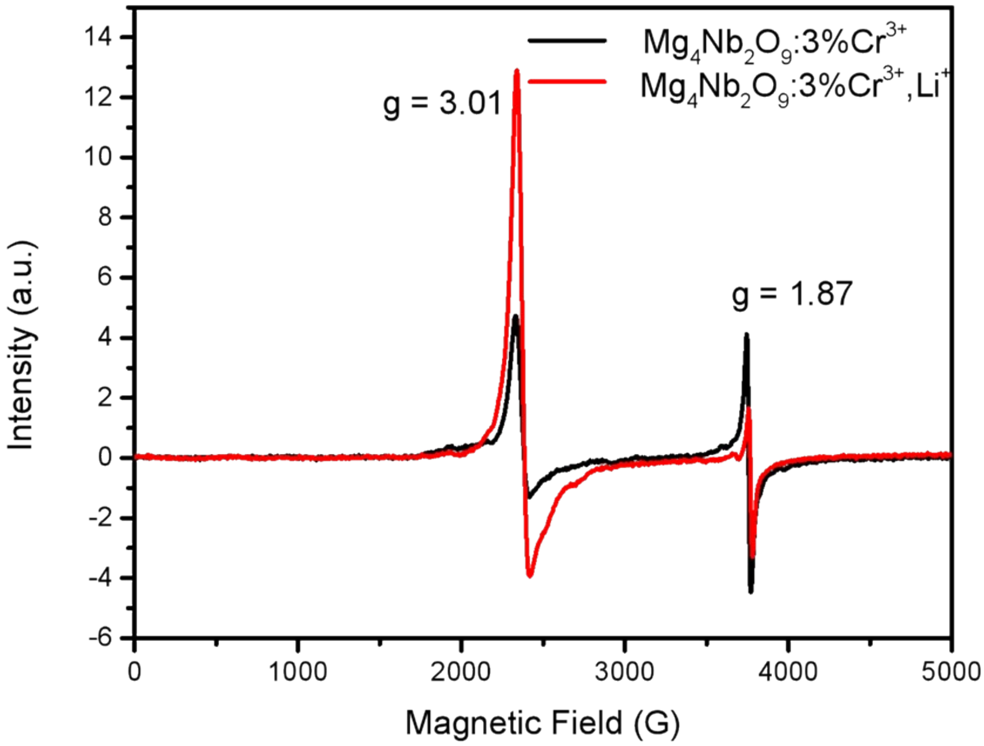

Fig. S11 EPR spectra of the $Mg_4Nb_2O_9$:3%Cr^{3+} and $Mg_4Nb_2O_9$:3%Cr^{3+},Li^{+} samples.

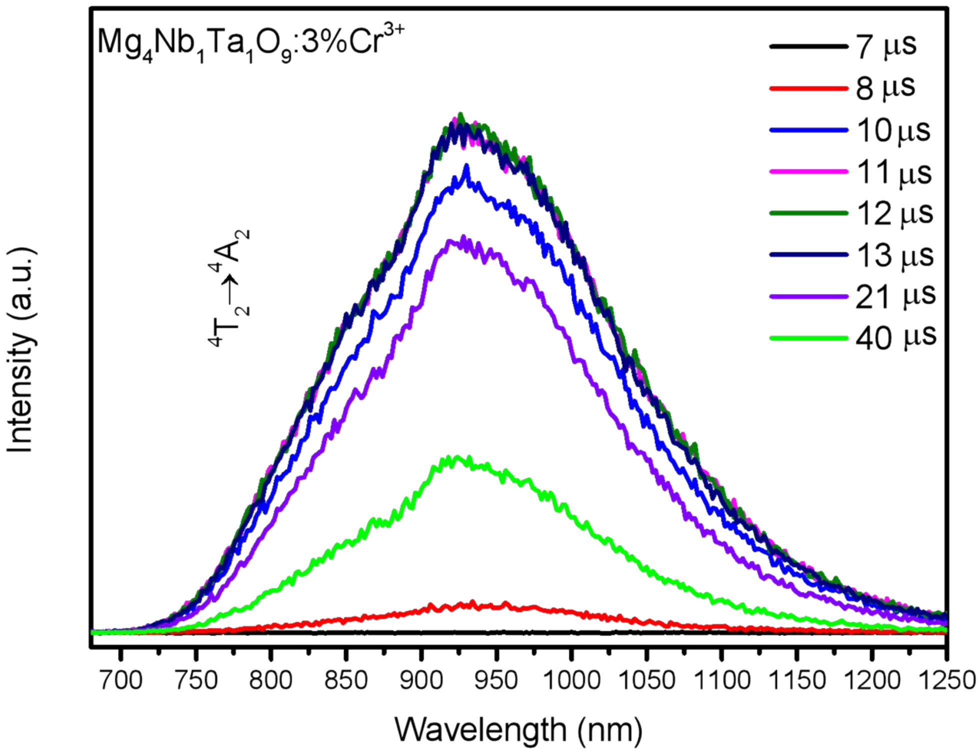

Fig. S12 Time-resolved emission spectra of the prepared $Mg_4Nb_1Ta_1O_9$:3%Cr^{3+} sample under pulsed light excitation of 468 nm.

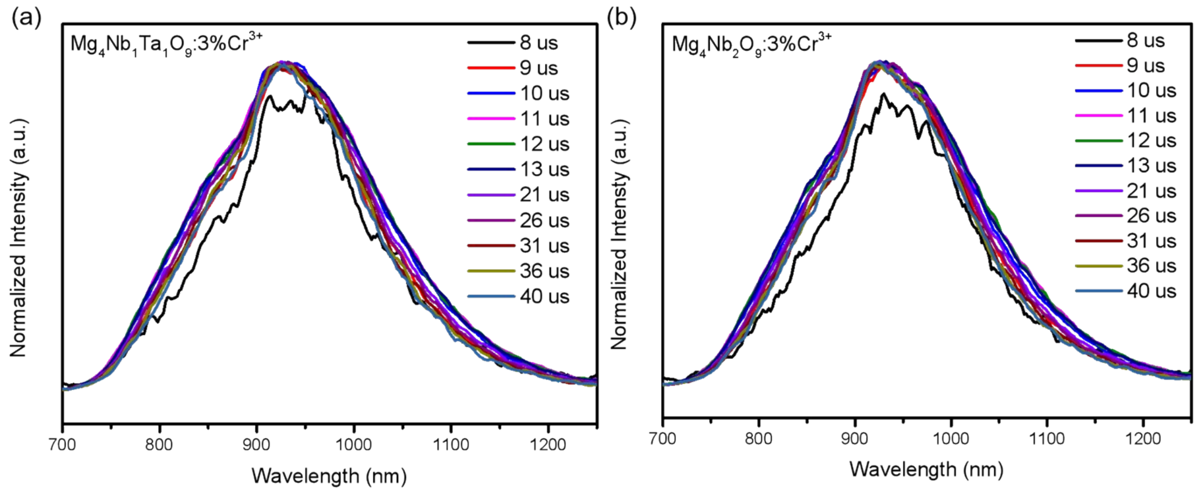

Fig. S13 Normalized time-resolved emission spectra of the (a) $Mg_4Nb_1Ta_1O_9$:3%Cr^{3+} and (b) $Mg_4Nb_2O_9$:3%Cr^{3+} samples under pulsed light excitation of 468 nm, respectively.

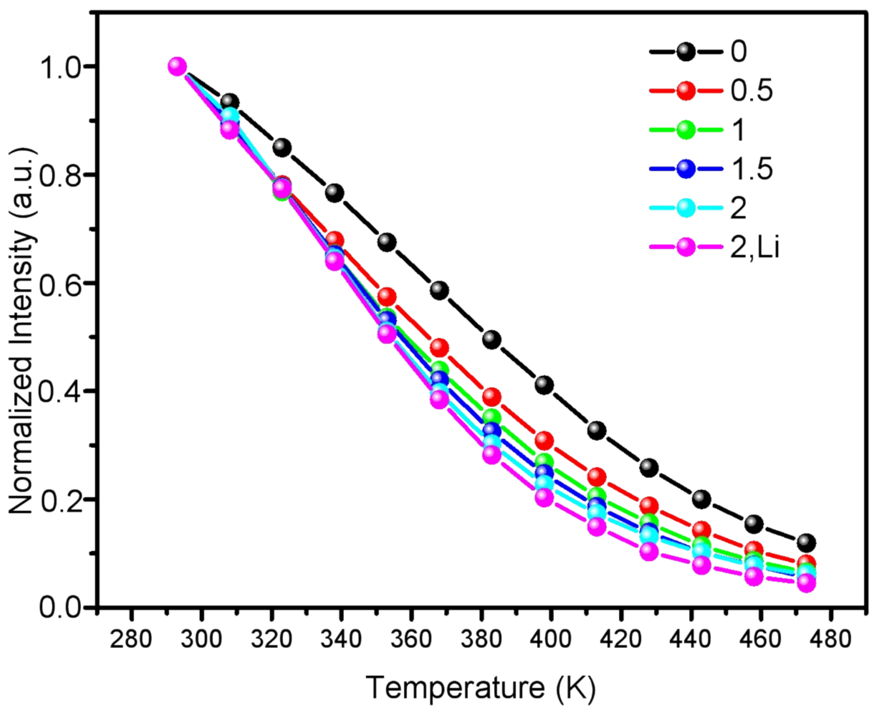

Fig. S14 Normalized PL intensities of $Mg_4Nb_xTa_{2-x}O_9$:3%Cr^{3+} (x = 0, 0.5, 1, 1.5, 2) samples and that of $Mg_4Nb_2O_9$:3%Cr^{3+},Li^+ sample as a function of temperature under excitation of 468 nm.

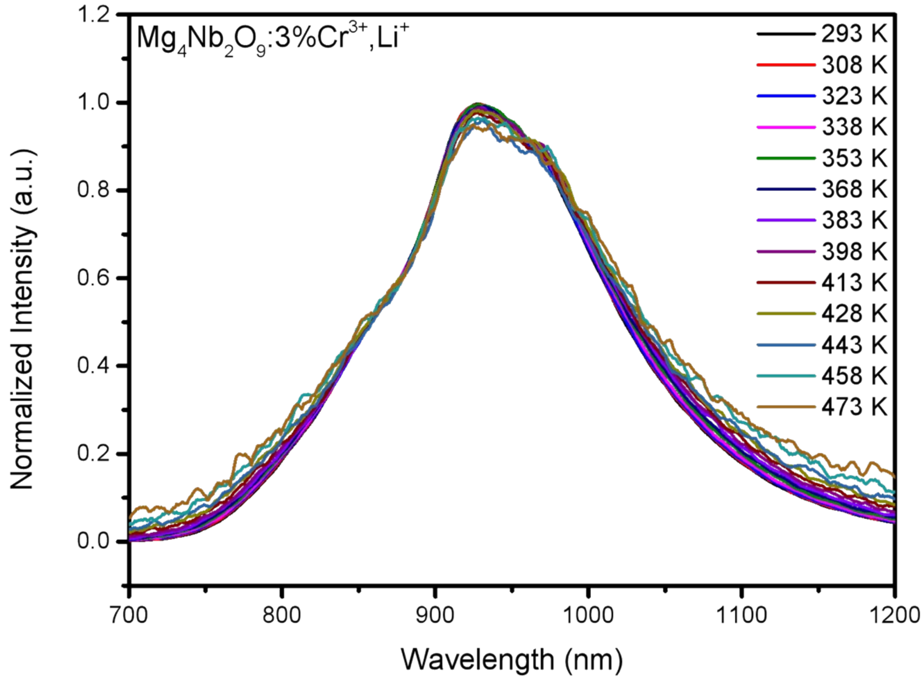

Fig. S15 Normalized PL spectra of the $Mg_4Nb_2O_9$:3%Cr^{3+},Li^+ sample upon 468 nm excitation as a function of temperature at a 15 K interval.

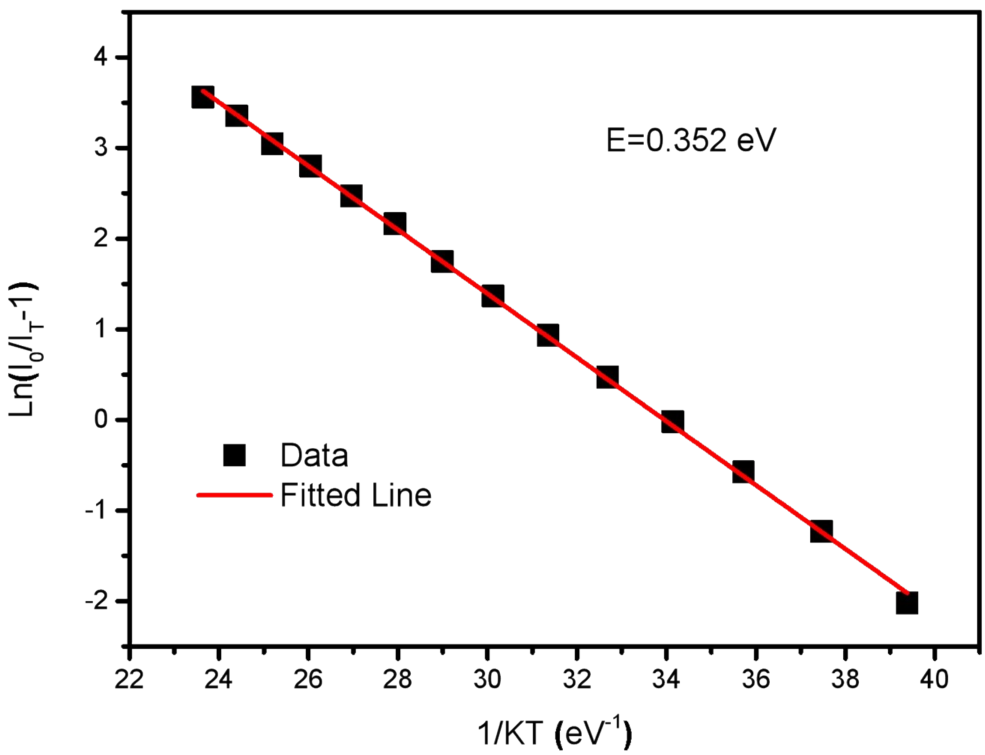

Fig. S16 $\mathrm{Ln}(I_0/I_T\!-\!1)$ versus 1/KT plot of the temperature dependent spectra ($I_0=I_{25°C}$)

Table S1. Rietveld refinement XRD of the as-synthesized $Mg_4Nb_xTa_{2-x}O_9$:3%Cr^{3+} (x = 0, 0.5, 1, 1.5, 2), and $Mg_4Nb_2O_9$:3%Cr^{3+},Li^+ polycrystalline powders

$Mg_4Ta_2O_9$:3%Cr^{3+}								
a	b	c	V	α	β	γ	R_{wp}	χ^2
5.164588	5.164588	14.060839	324.798	90	90	120	5.3290	2.66
$Mg_4Ta_{1.5}Nb_{0.5}O_9$:3%Cr^{3+}								
a	b	c	V	α	β	γ	R_{wp}	χ^2
5.162844	5.162844	14.050849	324.348	90	90	120	8.27	1.91
$Mg_4Ta_1Nb_1O_9$:3%Cr^{3+}								
a	b	c	V	α	β	γ	R_{wp}	χ^2
5.162246	5.162246	14.042261	324.075	90	90	120	8.71	1.96
$Mg_4Ta_{0.5}Nb_{1.5}O_9$:3%Cr^{3+}								
a	b	c	V	α	β	γ	R_{wp}	χ^2
5.159808	5.159808	14.031398	323.518	90	90	120	4.51	1.97
$Mg_4Nb_2O_9$:3%Cr^{3+}								
a	b	c	V	α	β	γ	R_{wp}	χ^2
5.15996	5.15996	14.025994	323.417	90	90	120	8.989	2
$Mg_4Nb_2O_9$:3%Cr^{3+},Li^+								
a	b	c	V	α	β	γ	R_{wp}	χ^2
5.160072	5.160072	14.02422	323.386	90	90	120	5.33	2.66

Table S2. The measured Internal QE, absorbance and External QE values of the $Mg_4Ta_2O_9$:3%Cr^{3+}, $Mg_4Nb_2O_9$:3%Cr^{3+} and $Mg_4Nb_2O_9$:3%Cr^{3+},Li^+ phosphor samples under excitation of 468 nm.

Phosphor sample	Internal QE	Absorbance	External QE
$Mg_4Ta_2O_9$:3%Cr^{3+}	0.561	0.339	0.19
$Mg_4Nb_2O_9$:3%Cr^{3+}	0.517	0.397	0.205
$Mg_4Nb_2O_9$:3%Cr^{3+},Li^+	0.671	0.389	0.261

Table S3 Mg-O bond length in $Mg_{3.97}Nb_xTa_{2-x}O_9$:3%Cr^{3+} (x = 0.5, 1, 1.5, 2) and $Mg_{3.97}Nb_xTa_{2-x}O_9$:3%Cr^{3+},Li^+ samples.

	x = 0	x = 0.5	x = 1	x = 1.5	x = 2	x = 2, Li
Mg1-O2^{I}	2.1798	2.3956	2.4402	2.1286	2.1472	2.1529
Mg1-O2^{II}	2.1802	2.3954	2.4404	2.1288	2.1468	2.1525
Mg1-O2^{III}	2.1800	2.3958	2.4406	2.129	2.147	2.1527
Mg1-O2^{IV}	2.1308	1.9383	1.881	2.0393	2.113	2.0727
Mg1-O2^{V}	2.1312	1.9381	1.8808	2.0389	2.1132	2.0725
Mg1-O2^{VI}	2.1310	1.9378	1.8806	2.0391	2.1127	2.073
D of Mg1-O	1.137%	10.558%	12.95%	2.15%	0.799%	2.035%
Mg2-O1^{I}	2.1575	2.1761	2.1988	1.991	2.069	2.0164
Mg2-O1^{II}	2.1579	2.1762	2.1985	1.9915	2.0687	2.0167
Mg2-O2^{III}	2.1577	2.1759	2.1989	1.9913	2.0692	2.0169
Mg2-O2^{IV}	2.0865	2.1043	2.1208	2.2151	2.2057	2.2177
Mg2-O2^{V}	2.0870	2.1044	2.1206	2.2147	2.2053	2.2175
Mg2-O2^{VI}	2.0868	2.1039	2.1203	2.2149	2.2056	2.2179
D of Mg2-O	1.671%	1.679%	1.89%	5.317%	2.035%	4.748%

The polyhedral distortion (D of Mg-O) can be evaluated by the following equation:

$$D = \frac{1}{n}\sum_{i=1}^{n}\frac{|D_i - D_{av}|}{D_{av}} \qquad \text{S1}$$

where n is the coordination numbers, D_i stands for the separation between the center cation and ith coordinating anions, D_{av} represents the average bond length.

Table S4. Fitting functions, R-square, and calculated decay time of the $Mg_4Nb_xTa_{2-x}O_9$:3%Cr^{3+} (x = 0, 0.5, 1, 1.5, 2) and $Mg_4Nb_2O_9$:3%Cr^{3+},Li^+ phosphors under pulsed light excitation of 468 nm.

Sample	fitting function	decay time/μs	R-square
$Mg_4Ta_2O_9$:3%Cr^{3+}	$I=A1*\exp(-t/\tau) + y_0$	$\tau \sim 22.7$	0.99868
$Mg_4Nb_{0.5}Ta_{1.5}O_9$:3%Cr^{3+}	$I=A*\exp(-t/\tau) + y_0$	$\tau \sim 21.7$	0.99868
$Mg_4Nb_1Ta_1O_9$:3%Cr^{3+}	$I=A*\exp(-t/\tau) + y_0$	$\tau \sim 20.4$	0.99901
$Mg_4Nb_{1.5}Ta_{0.5}O_9$:3%Cr^{3+}	$I=A*\exp(-t/\tau) + y_0$	$\tau \sim 20.2$	0.99894
$Mg_4Nb_2O_9$:3%Cr^{3+}	$I=A*\exp(-t/\tau) + y_0$	$\tau \sim 19.5$	0.999
$Mg_4Nb_2O_9$:3%Cr^{3+},Li^+	$I=A*\exp(-t/\tau) + y_0$	$\tau \sim 20.0$	0.99

Table S5. PL peak (λ_{em}) and PLE peak (λ_{ex}) wavelengths, FWHM value, internal QE (IQE) and external QE (EQE), thermal stability of our prepared sample versus some reported Cr^{3+}-doped long-wave broadband NIR phosphors, as well as the corresponding photoelectric performance of fabricated *pc*-LED devices.

Hosts	λ_{ex} nm	λ_{em} nm	FWHM nm	IQE %	EQE %	Thermal stability	NIR output power	Photoelectric efficiency	Ref
$Mg_4Nb_2O_9$: 3%Cr^{3+},Li^+	465	920	167	67.1	26.1	32.3%@ 368K	5.1 mW@ 20 mA	10.3%@20 mA	This work
$GaTaO_4$: 0.6%Cr^{3+}	460	840	140	91	\	85%@ 373K	178 mW@ 500 mA	6%@500 mA	1
$Mg_4Ta_2O_9$: 3%Cr^{3+}	460	850	188	72	33.4	58.4%@ 373K	60.9 mW@ 150mA	22.1%@10 mA	2
$Mg_4Ta_2O_9$: 3%Cr^{3+}	450	842	167	\	61.2 5	55%@ 373K	53.22 mW @100 mA	25.09%@10 mA	3
$Mg_4Ta_2O_9$: 1%Cr^{3+}	460	850	178	\	\	82%@ 423K	11.33 mW @300 mA	\	4
$ZnTa_2O_6$: 4%Cr^{3+}	480	935	185	24.5	13.5	49%@ 373K	39.8 mW@ 300 mA	4.2%@300 mA	5
$MgTa_2O_6$: 2.1%Cr^{3+}	460	834	140	\	\	\	\	\	6
$InTaO_4$: 4%Cr^{3+}	500	839	125	\	\	~23%@ 360 K	\	\	7
$GaTa_{0.5}Nb_{0.5}O_4$:2.5%Cr^{3+}	476	865	145	94	\	55.5%@ 450K	42.5 mW @20 mA	9.37%@20 mA	8
$ScTaO_4$: 2%Cr^{3+}	516	940	186	\	\	~16%@ 373 K	\	\	9
$Cs_2AgInCl_6$: 10%Cr^{3+}	405	101 0	180	22.0 3	\	~10%@ 373 K	\	\	10
$LiIn_2SbO_6$:Cr^{3+}:3%Cr^{3+}	492	970	225	7	3.4	10%@3 68K	\	\	11
$LiScP_2O_7$: 6%Cr^{3+}	470	880	170	38	20	41%@ 373 K	19 mW@ 100 mA	7%@100 mA	12
$Li_3Sc_2(PO_4)_3$: 8%Cr^{3+}	496	978	240	\	\	37%@3 73K	5.81mW@ 80mA	2.62%@80 mA	13

References:

1 J. Zhong, Y. Zhuo, F. Du, H. Zhang, W. Zhao, S. You and J. Brgoch, *Adv. Opt. Mater.*, 2022, **10**, 2101800.

2 W. Tang, D. Wu, Y. Xiao, X. Dong, Y. Wang, W. Zhou, Y. Liu and L. Zhang, *Adv. Opt. Mater.*, 2022, **11**, 2202237.

3 S. Wang, R. Pang, T. Tan, H. Wu, Q. Wang, C. Li, S. Zhang, T. Tan, H. You and H. Zhang, *Adv. Mater.*, 2023, **35**, 2300124.

4 X. Ding, Y. Min, C. Wang and Q. Zhang, *Infrared Phys. Techn.*, 2023, **131**, 104697.

5 S. He, P. Li, Y. Ren, G. Wei, Y. Wang, Y. Yang, R. Li, J. Li, Y. Shi, X. Shi and Z. Wang, *Inorg. Chem.* 2022, **61**, 11284-11292.

6 G. Liu, M. Molokeev, B. Lei and Z. Xia, *J. Mater. Chem. C* 2020, **8**, 9322-9328.

7 L. Qiu, P. Wang, J. Mao, Z. Liao, F. Chi, Y.Chen, X. Wei and M. Yin, *Inorg. Chem. Front.*, 2022, ***9***, 3187-3199.

8 S. Liu, G. Wang, L. Xu, H. Jia, X. Sun and H. Yuan, *Ceram. Int.*, 2023, **49**, 33401-33406.

9 S. Wang, S. Zhang, S. Liu, S. Han, X. Li, C. Wang and C. Li, *Dalton. Trans.*, 2022, **51**, 16325-16335.

10 F. Zhao, Z. Song, J. Zhao and Q. Liu, *Chem. Front.*, 2019, **6**, 3621-3628.

11 G. Liu, T. Hu, M. Molokeev and Z. Xia, *iScience* 2021, **24**, 102250.

12 L. Yao, Q. Shao, S. Han, C. Liang, J. He and J. Jiang, *Chem. Mater.*, 2020, **32**, 2430-2439.

13 S. Zhao, L. Lou, S. Yuan, D. Zhu, F. Wu and Z. Mu, *J. Lumin.*, 2022, **251**, 119188.